Experimental and theoretical study of the crystal-field levels and hyperfine and electron-phonon interactions in $LiYF_4:Er^{3+}$

M. N. Popova and E. P. Chukalina

Institute of Spectroscopy, Russian Academy of Sciences, 142092 Troitsk, Moscow region, Russia

B. Z. Malkin and S. K. Saikin

Kazan State University, 420008 Kazan, Russia

We have measured high resolution absorption spectra for the $^4I_{15/2} \rightarrow {}^4I_{13/2}, {}^4I_{11/2}$ infrared transitions of Er^{3+} ions in $LiYF_4$. Positions of crystal-field levels and their widths were precisely determined and analyzed. Hyperfine structure of ^{167}Er totaling ~ 0.2 cm^{-1} was observed. Experimental data are described by a theory that operates with a realistic model of the lattice dynamics and with the crystal-field parameters and electron-phonon coupling constants calculated in the framework of the exchange charge model. The hyperfine splittings of the odd mass number isotope ^{167}Er are calculated taking into account both magnetic dipole and electric quadrupole hyperfine interactions. The simulated hyperfine structure is in good agreement with the experimentally observed one. The one-phonon relaxation rates within the $^4I_{11/2}$ and $^4I_{13/2}$ crystal-field manifolds are calculated using the correlation functions of the Er^{3+} ion and ligand displacements. The results of these calculations agree within an order of magnitude with the measured homogeneous linewidths of the corresponding zero-phonon transitions from the ground state at low temperatures.

I. INTRODUCTION

The scheelite crystal $LiYF_4$ doped with Er^{3+} ions is well known as an efficient multifrequency laser material (see, e.g., Refs. 1,2, and references therein). Laser action at 2.7 μm that occurs between the excited $^4I_{11/2}$ and $^4I_{13/2}$ multiplets has attracted particular interest because of applications in long distance transmission by optical fibers. A detailed knowledge of the energy levels within the $^4I_{11/2}$ and $^4I_{13/2}$ multiplets is important for a better understanding of the laser characteristics.

Though the crystal-field splittings of the energy levels of Er^{3+} in $LiYF_4$ have been extensively studied,[1,3–9] there exists a great discrepancy (up to 40 cm^{-1}) between the data of different authors concerning the $^4I_{13/2}$ and, especially, the $^4I_{11/2}$ multiplets. The widths of many lines in the infrared spectra reported in the works mentioned above were limited by an instrumental resolution of, typically, several wave numbers. It is worth mentioning here that our earlier works on the spectra of another rare-earth ion, Ho^{3+}, in $LiYF_4$ revealed inhomogeneously broadened lines as narrow as 0.007 cm^{-1}, hyperfine structure with typical extent of 1 cm^{-1},[10] and fine structure (0.01–0.03 cm^{-1}) within each hyperfine component due to isotopic disorder in the lithium sublattice.[11] The only high-resolution study of $LiYF_4:Er^{3+}$ (isotopically purified in Li) concerned one spectral line in the visible, namely, the 15 302.4 cm^{-1} line of the $^4I_{15/2} \rightarrow {}^4F_{9/2}$ transition.[12] Hyperfine structure of ^{167}Er extending over 0.2 cm^{-1} and isotope structure due to even mass number isotopes of Er totaling 0.01 cm^{-1} were found.

The purpose of this work was to precisely determine the positions of crystal-field levels of the $^4I_{13/2}$ and $^4I_{11/2}$ multiplets and to study the linewidths of the $^4I_{15/2} \rightarrow {}^4I_{13/2}, {}^4I_{11/2}$ transitions, paying special attention to the relaxation broadening, with the aim of checking the validity of the previously developed theoretical model of the electron-phonon interaction[13] for calculation of phonon relaxation rates. The crystal-field energies of Er^{3+} ions, hyperfine splittings, and relative intensities of transitions between electronic-nuclear sublevels of ^{167}Er isotope are calculated and compared with the experimental data. The electron-phonon coupling constants are calculated in the framework of the exchange charge model with parameters fitted to the measured crystal-field splittings. Probabilities of the one-phonon transitions within the crystal field multiplets $^4I_{13/2}$ and $^4I_{11/2}$, which determine the homogeneous linewidths of absorption lines in spectra of even Er isotopes, have been estimated, with the correlation functions of the Er^{3+} ion and ligand displacements obtained in the framework of a realistic model of the vibrational spectrum of the $LiYF_4$ crystal lattice.

II. EXPERIMENTAL PROCEDURE

We studied 0.2% Er^{3+}-doped $LiYF_4$ crystals with natural abundance of lithium and erbium isotopes. Several measurements were performed on samples of $LiYF_4:Er^{3+}$ (3.5%) and $LiErF_4$. Crystals were grown by the Czochralski method and were oriented along the c axis. Transmission spectra were measured at temperatures between 5 K and 60 K in the region of the $^4I_{15/2} \rightarrow {}^4I_{13/2}, {}^4I_{11/2}$ transitions (frequency ranges about 6600 cm^{-1} and 10 200 cm^{-1}) with a spectral resolution up to 0.005 cm^{-1}. The absolute precision of the wave number scale was about 0.002 cm^{-1}. The spectra were obtained using a BOMEM DA3.002 high-resolution Fourier-transform spectrometer. The method of Fourier-transform spectroscopy ensures a high resolution in a broad spectral range and a high absolute precision of the wave number scale.
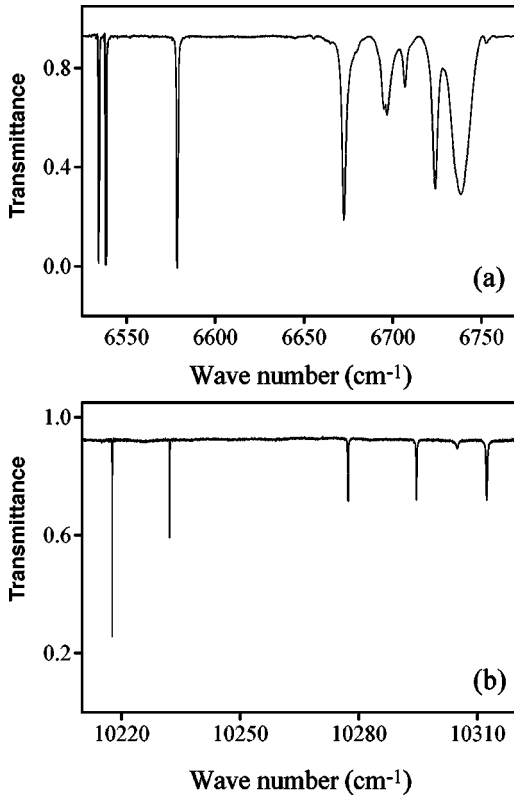
FIG. 1. Transmittance spectra of $LiYF_4:Er^{3+}$ (0.2%) at 5 K in the region of the transitions (a) $^4I_{15/2} \rightarrow ^4I_{13/2}$ and (b) $^4I_{15/2} \rightarrow ^4I_{11/2}$. $\mathbf{E,H} \perp c$ polarization.

III. EXPERIMENTAL RESULTS

Spectra corresponding to the $^4I_{15/2} \rightarrow ^4I_{13/2}, ^4I_{11/2}$ transitions are presented in Fig. 1. Table I lists the energies of the crystal-field levels of the $^4I_{15/2}$, $^4I_{13/2}$, and $^4I_{11/2}$ multiplets.

If not otherwise indicated, the accuracy of the level positions is better than $\pm 0.05 \, \text{cm}^{-1}$. The positions of the levels change little with changing erbium concentration. We checked that the three lowest-energy levels of the $^4I_{13/2}$ multiplet in $LiErF_4$ shift by no more than 0.4 cm^{-1} from their positions in $LiYF_4:Er(0.2\%)$. Such behavior is in agreement with the results of our earlier study of another erbium system, $(Y_{1-x}Er_x)Al_5O_{12}$. We found that the level positions in the $^4I_{13/2}$ multiplet depend linearly on x, the total change being less than 0.9 cm^{-1} for the whole interval of x between 0.001 and 1.0.[14] The total crystal-field splittings of the $^4I_{13/2}$ and $^4I_{11/2}$ levels of Er^{3+} in $LiYF_4$ are 204 and 95 cm^{-1}, respectively. Close values of splittings (193–214 cm^{-1} for the $^4I_{13/2}$ level and 95–102 cm^{-1} for the $^4I_{11/2}$ level) were observed in the case of Er^{3+} in LaF_3 and tungstates with scheelite structure, whereas greater values (297–336 and 135–163 cm^{-1}) have been reported for Er^{3+} in garnets.[15]

For the $^4I_{13/2}$ multiplet, the data of Kulpa[4] and Petrov and Tkachuk[1] coincide within 1 cm^{-1} with ours, while the energies reported by Couto dos Santos et al.[9] are shifted by 4–8 cm^{-1} to the higher-energy side. For the $^4I_{11/2}$ multiplet, Kulpa[4] reported, correctly, only the lowest level. The data of Ref. 1 are shifted by 4–8 cm^{-1} to the higher side and the level 10 305 cm^{-1} is misplaced to 10 355 cm^{-1}. The accuracy of the energies reported in Ref. 9 varies from -4 to 15 cm^{-1}. The crystal-field splittings of both the $^4I_{13/2}$ and $^4I_{11/2}$ levels communicated by Hubert et al.[7] and by Auzel and Chen[8] agree within 1 cm^{-1} with our data when temperature corrections are taken into account. Many of the level positions reported by Christensen[5] from low-resolution and saturated spectra of the $^4I_{15/2} \rightarrow ^4I_{13/2}, ^4I_{11/2}$ transitions of $LiErF_4$ came from erroneous assignments of spectral lines originating from excited levels of the ground multiplet.

TABLE I. Measured and calculated positions (E) and widths (ΔE) of the crystal-field levels in $LiYF_4:Er^{3+}$ (0.2%) at 5 K.

Multiplet	Γ	E (cm^{-1})		ΔE (cm^{-1})	
		Experiment	Theory	Experiment	Theory ($\times 3$)
$^4I_{11/2}$	$\Gamma_{78}^{(3)}$	10312.4	10321	0.35	0.53
	$\Gamma_{78}^{(2)}$	10305.6	10310	0.76	0.89
	$\Gamma_{56}^{(3)}$	10294.6	10303	0.21	0.85
	$\Gamma_{56}^{(2)}$	10277.3	10285	0.20	0.76
	$\Gamma_{56}^{(1)}$	10232.2	10237	0.018	0.005
	$\Gamma_{78}^{(1)}$	10217.6	10218	0.016	0
$^4I_{13/2}$	$\Gamma_{56}^{(4)}$	6738.3±0.3	6736	7.0	6.16
	$\Gamma_{78}^{(3)}$	6724.0	6719	2.7	2.70
	$\Gamma_{56}^{(3)}$	6696.0	6699	2.5	2.97
	$\Gamma_{78}^{(2)}$	6672.5	6669	2.0	2.12
	$\Gamma_{56}^{(2)}$	6578.6	6582	0.07	0.086
	$\Gamma_{56}^{(1)}$	6538.3	6538	0.017	0.0002
	$\Gamma_{78}^{(1)}$	6534.3	6534	0.015	0
$^4I_{15/2}$	$\Gamma_{78}^{(2)}$	56.0 [a]	55		
	$\Gamma_{56}^{(2)}$	27.6 [a]	20		
	$\Gamma_{78}^{(1)}$	17.0 [a]	15		
	$\Gamma_{56}^{(1)}$	0	0		

[a]At 60 K.

FIG. 2. Absorption lines of $LiYF_4:Er^{3+}(0.2\%)$ at 5 K corresponding to the transitions (a) $^4I_{15/2}(\Gamma_{56}^{(1)}) \rightarrow {}^4I_{13/2}(\Gamma_{78}^{(1)})$, (b) $^4I_{15/2}(\Gamma_{56}^{(1)})$ $\rightarrow {}^4I_{13/2}(\Gamma_{56}^{(1)})$, (c) $^4I_{15/2}(\Gamma_{56}^{(1)}) \rightarrow {}^4I_{11/2}(\Gamma_{78}^{(1)})$, and (d) $^4I_{15/2}(\Gamma_{56}^{(1)}) \rightarrow {}^4I_{11/2}(\Gamma_{56}^{(1)})$. $\mathbf{E,H} \perp c$ polarization. Spectral resolution equals 0.01 cm^{-1}. Calculated hyperfine structure due to $^{167}Er^{3+}$ is shown by sticks whose heights are proportional to the relative intensities of hyperfine components.

Low-frequency lines of each multiplet are narrow, several hundredths of wave number wide (see Table I). This is in contrast with the much wider (several tenths of a wave number) inhomogeneously broadened lines of Er^{3+} in yttrium aluminum garnet.[14] The main cause of inhomogeneous line broadening in garnets is the presence of point defects of the type ''yttrium at the aluminum site.'' Due to the large difference in ionic radii between Y^{3+} and Al^{3+}, these defects create strong local strains. Evidently, defects of this type are absent in $LiYF_4$ crystals that grow at appreciably lower temperatures ($\sim1100\,°C$) than garnets ($\sim1900\,°C$). Figure 2 displays the four narrowest lines in the spectrum of $LiYF_4:Er$ (0.2%). Multiple weak lines are present at both sides of the main line. A line shape does not change when the Er concentration is increased up to 3.5%; the lines broaden and new lines with intensity quadratic in concentration appear outside the spectral region displayed in Fig. 2.

The widths of the main lines in Fig. 2 contain unresolved isotope shifts induced both by even number mass isotopes of Er and by ^6Li isotopes of the lattice[11,12] (we shall discuss isotope effects elsewhere). The weak lines are due to the hyperfine structure of the ^{167}Er (nuclear spin $I=7/2$) levels.[12] Since even-even nuclei have zero spin in the ground state, the other even erbium isotopes do not contribute to the hyperfine structure of the spectral lines.

The hyperfine structure of the ^{167}Er spectrum is not resolved in the high-frequency lines of each spectral manifold, which are broadened by the phonon relaxation. The corresponding linewidths (see Table I) correlate with the crystal-

field energies and vary from several tenths of a wave number in the $^4I_{11/2}$ multiplet up to several wave numbers in the $^4I_{13/2}$ multiplet.

IV. THEORY AND DISCUSSION

A. Crystal-field energies and hyperfine interactions

The energy level pattern of the $^{167}Er^{3+}$ ion (22.9% abundant) in the crystal field can be represented by eigenvalues of the effective parametrized Hamiltonian

$$H = H_0 + H_{cf} + H_{hf}, \qquad (1)$$

where H_0 corresponds to the free ion energy renormalized by the symmetrical component of the crystal field, H_{cf} is the crystal-field Hamiltonian, and H_{hf} is the nuclear energy responsible for the hyperfine structure in the optical spectra. To obtain the energy levels of Er even isotopes, we use the same Hamiltonian (1) omitting H_{hf}. In the $LiYF_4$ lattice, trivalent rare-earth ions substitute for Y^{3+} ions in sites of S_4 symmetry and the crystal-field Hamiltonian can be presented in the crystallographic system of coordinates by seven crystal-field parameters B_p^k:

$$H_{cf} = B_2^0 O_2^0 + B_4^0 O_4^0 + B_4^4 O_4^4 + B_4^{-4} O_4^{-4} + B_6^0 O_6^0 + B_6^4 O_6^4$$
$$+ B_6^{-4} O_6^{-4}, \qquad (2)$$

where O_p^k (Stevens operators) are the linear combinations of the spherical operators C_k^p:

$$a_{p|k|}O_p^{|k|} = C_{-|k|}^p + (-1)^k C_{|k|}^p, \quad a_{p0}O_p^0 = C_0^p,$$

$$a_{p|k|}O_p^{-|k|} = i[C_{-|k|}^p - (-1)^k C_{|k|}^p]. \tag{3}$$

Numerical factors a_{pk} are presented in Ref. 13 (in particular, $a_{20}=1/2$, $a_{40}=1/8$, $a_{60}=1/16$, $a_{44}=\sqrt{70}/8$, $a_{64}=\sqrt{126}/16$). The quantization axis z coincides with the symmetry axis of the crystal lattice. In the present work, only the low-lying multiplets of the $4f^{11}$ electronic shell of the Er^{3+} ion are considered, so we restrict ourselves to explicit calculations of matrix elements of the Hamiltonian (1) in the space of electronic wave functions belonging to the lowest ^4I and the first excited ^4F manifolds. For the $^4I_{15/2}$, $^4I_{13/2}$, and $^4I_{11/2}$ multiplets the J mixing effect is small, and we can take into account only projections of the electron-nuclear magnetic and quadrupolar interactions on multiplets with fixed electronic orbital (L), spin (S), and total (J) angular moments:

$$H_{hf} = A(L,S)_J\, \mathbf{J}\cdot\mathbf{I} + \frac{e^2 Q(1-\gamma)}{4I(2I-1)} V_{zz} [3I_z^2 - I(I+1)]$$

$$+ \frac{3C\,[\alpha(L,S,J)/\alpha(^4I_{15/2})]}{4I(2I-1)J(2J-1)} \left\{ \frac{1}{3}[3J_z^2 - J(J+1)] \right.$$

$$\times [3I_z^2 - I(I+1)] + \frac{1}{2}(J_+^2 I_-^2 + J_-^2 I_+^2)$$

$$+ \frac{1}{2}(J_z J_+ + J_+ J_z)(I_z I_- + I_- I_z)$$

$$\left. + \frac{1}{2}(J_z J_- + J_- J_z)(I_z I_+ + I_+ I_z) \right\}. \tag{4}$$

Here $A(L,S)_J$ are the magnetic dipole hyperfine constants. For the ground state of the Er^{3+} ion, $A(^4I_{15/2}) = -0.00418$ cm^{-1};[16,17] the corresponding hyperfine constants for other multiplets are obtained using this value and neglecting the core electron polarization contributions which do not exceed 1.5% of the $4f$ electron contributions,[18] in particular, $A(^4I_{13/2}) = -0.0049$ cm^{-1} and $A(^4I_{11/2}) = -0.00546$ cm^{-1}. The nuclear quadrupole moment $Q = 283 \times 10^{-30}$ m^2,[17] $\gamma = -70$ is the Sternheimer antishielding factor,[19] the constant C of the intraionic quadrupole interaction in the ground state equals -0.0635 cm^{-1},[17] and $\alpha(L,S,J)$ are reduced matrix elements of the second rank spherical operators. The ionic lattice contribution to the electric field gradient at the Er^{3+} nucleus is given by

$$eV_{zz} = \sum_s eq_s \frac{3\cos^2\theta_s - 1}{R_s^3}, \tag{5}$$

where q_s is the charge (in units of the proton charge e) of a lattice ion with spherical coordinates R_s, θ_s, and φ_s in the system of coordinates having its origin at the Er^{3+} nucleus. The lattice sum (5) was calculated using the Ewald method and effecive ion charges of $-0.9e$ (F$^-$), $0.9e$ (Li$^+$), $2.7e$ (Y^{3+}),[20,21] and we obtained $e^2 Q(1-\gamma)V_{zz} = -0.00365$ cm^{-1}.

The crystal-field parameters for Er^{3+} in LiYF$_4$ were obtained in Ref. 22 from the fit of the calculated crystal-field splittings to the experimental data (see Table II, column 3). Due to the initially imposed constraint $B_4^{-4}=0$, this set of

TABLE II. Crystal-field parameters B_p^k in LiYF$_4$:Er^{3+} (in cm^{-1}).

p	k	Contributions from the first coordination shell calculated with the ECM	Ref. 22	Ref. 20
1		2	3	4
2	0	260	190	190
4	0	−77.4	−80	−80
4	4	−622	−1020	−771
4	−4	−640	0	−667
6	0	−2.2	−2.3	−2.3
6	4	−258	−420	−363
6	−4	−206	70	−222

parameters cannot be related to the crystallographic axes. Similarly to Ref. 20, we use here the set of crystal-field parameters given in column 4 of Table II, which have been obtained from the empirical parameters[22] by a rotation of the coordinate system about the z axis through an angle determined on the basis of the relation between the B_4^4 and B_4^{-4} parameters calculated in the framework of the semiphenomenological exchange charge model (ECM).[13] Such a transformation is necessary to derive wave functions of the crystal-field states related to the real structure of the crystal lattice. The numerical diagonalization of the matrix of the Hamiltonian $H_0 + H_{cf}$, which has a dimension of 80 in the $|LSJJ_z\rangle$ representation ($S=3/2$; L = 3, 6), with the fitted multiplet baricenters of 0 ($^4I_{15/2}$), 6485.5 ($^4I_{13/2}$), 10 122 ($^4I_{11/2}$), 12 368.3 ($^4I_{9/2}$), 15 210 ($^4F_{9/2}$), 20 487 ($^4F_{7/2}$), 22 134 ($^4F_{5/2}$), and 22 475 ($^4F_{3/2}$) cm^{-1} results in crystal-field energies of the Er^{3+} ion (even isotopes) that agree satisfactorily with the experimental data (see Table I; the root-mean-square deviation is 4.7 cm^{-1}). Energies and wave functions of the mixed electronic-nuclear states of the $^{167}Er^{3+}$ ion were obtained by the numerical diagonalization of the total matrix (640×640) of the Hamiltonian (1) where the hyperfine interaction was represented by quasidiagonal blocks of $(2I+1)(2J+1)$ dimensionality. Relative intensities of the optical transitions between the electronic-nuclear sublevels of the ground doublet $^4I_{15/2}(\Gamma_{56}^{(1)})$ and sublevels of the excited multiplets, induced by the radiation propagating along the c axis of crystal, were computed as squared matrix elements of the effective electric dipole moment of the Er^{3+} ion using eigenfunctions of the Hamiltonian (1). It should be noted that in the radiation field with the $\mathbf{E},\mathbf{H} \perp c$ polarization, magnetic dipole transitions, when they are allowed, do not change the relative intensities of hyperfine components of an individual electric dipole transition between crystal field levels. Components of the electric dipole moment along the crystallographic axes in the lattice basis plane can be represented by the operators

$$D_x = b_2^1 O_2^1 + b_4^1 O_4^1 + b_4^3 O_4^3 + b_6^1 O_6^1 + b_6^3 O_6^3 + b_6^5 O_6^5 + b_2^{-1} O_2^{-1}$$

$$+ b_4^{-1} O_4^{-1} + b_4^{-3} O_4^{-3} + b_6^{-1} O_6^{-1} + b_6^{-3} O_6^{-3} + b_6^{-5} O_6^{-5}, \tag{6}$$

$$D_y = b_2^{-1}O_2^1 + b_4^{-1}O_4^1 - b_4^{-3}O_2^3 + b_6^{-1}O_6^1 - b_6^{-3}O_6^3 + b_6^{-5}O_6^5$$
$$- b_2^1 O_2^{-1} - b_4^1 O_4^{-1} + b_4^3 O_4^{-3} - b_6^1 O_6^{-1} + b_6^3 O_6^{-3}$$
$$- b_6^5 O_6^{-5}, \tag{7}$$

defined to operate intraconfigurationally. Parameters b_p^k were calculated taking into account mixing of the $4f$ and $5d$ electronic states of the Er^{3+} ion due to odd components of the crystal field and the lattice polarization in the radiation field. The following values of b_p^k were obtained: $b_2^1 = 6.2$, $b_2^{-1} = -7.7$, $b_4^1 = -8.5$, $b_4^{-1} = 18.1$, $b_6^1 = 2.7$, $b_6^{-1} = -6.2$, $b_4^3 = 20.8$, $b_4^{-3} = -25.6$, $b_6^3 = -6.5$, $b_6^{-3} = 18.9$, $b_6^5 = -28.8$, $b_6^{-5} = 4.6$ (in units of 10^{-4} e nm). We omit here details of the calculations because the relative intensities of hyperfine components of a given spectral line are only slightly dependent on the relative values of the b_p^k parameters. The simulated hyperfine splittings of the four spectral lines with the experimentally resolved hyperfine structure $[{}^4I_{15/2}(\Gamma_{56}^{(1)}) \to {}^4I_{13/2}(\Gamma_{78}^{(1)}), {}^4I_{13/2}(\Gamma_{56}^{(1)}), {}^4I_{11/2}(\Gamma_{78}^{(1)}), {}^4I_{11/2}(\Gamma_{56}^{(1)})]$ and the relative intensities of the corresponding hyperfine components, presented by sticks in Fig. 2, agree within 10% with those observed in the absorption spectrum.

B. One-phonon relaxation rates and linewidths

The Hamiltonian of the electron-phonon interaction, linear in displacements of ions from their equilibrium positions in the lattice, and correspondingly linear in phonon creation and annihilation operators, can be written as follows:

$$H_{el-ph} = \sum_{s\alpha} V_\alpha(s)[u_\alpha(s) - u_\alpha(Er)];$$

$$V_\alpha(s) = \sum_{pk} B_{p,\alpha}^k(s) O_p^k, \tag{8}$$

where $\mathbf{u}(s) - \mathbf{u}(Er)$ is the difference between dynamic displacements of the ligand ion s and the Er^{3+} ion, $\alpha = x, y, z$, and $B_{p,\alpha}^k(s)$ are the coupling constants. Values of the coupling constants were computed in the framework of the ECM with the same parameters as those used in the crystal-field calculations. Earlier this model was successfully used when analyzing magnetoelastic properties of LiErF$_4$,[20] spin-lattice relaxation rates,[23] and piezospectroscopic effects[24] in LiYF$_4$:Er^{3+}. The crystal field is represented by a sum of the electrostatic field of point charges of lattice ions and the exchange charge field; the corresponding contributions to the coupling constants

$$B_{p,\alpha}^k(s) = B_{p,\alpha}^{(pc)k}(s) + B_{p,\alpha}^{(ec)k}(s) \tag{9}$$

equal

$$B_{p,\alpha}^{(pc)k}(s) = e^2 q_s (p+1) K_{pk} (1 - \sigma_p)$$
$$\times \langle r^p \rangle \frac{a_{p+1,0}}{a_{p,0}} \frac{W_{p,\alpha}^k(\theta_s, \varphi_s)}{R_s^{p+2}}, \tag{10}$$

$$B_{p,\alpha}^{(ec)k}(s) = -\frac{2(2p+1)}{7R_s^2} K_{pk} e^2$$
$$\times \left[(p+1) \frac{a_{p+1,0}}{a_{p,0}} W_{p,\alpha}^k(\theta_s, \varphi_s) S_p(R_s) \right.$$
$$\left. - R_{s,\alpha} O_p^k(\theta_s, \varphi_s) \left(p \frac{S_p(R_s)}{R_s} + \frac{d}{dR_s} S_p(R_s) \right) \right]. \tag{11}$$

Here $K_{pk} = a_{pk}^2/2$ $(k \neq 0)$, $K_{p0} = a_{p0}^2$; σ_p are the shielding factors $[\sigma_2 = 0.44, \sigma_4 = \sigma_6 = 0$ (Ref. 25)$]$, and $\langle r^p \rangle$ are moments of the radial wave function of the $4f$ electron calculated in Ref. 26 (for the Er^{3+} ion, $\langle r^2 \rangle = 0.666$, $\langle r^4 \rangle = 1.126$, $\langle r^6 \rangle = 3.978$, in atomic units).

$$S_p(R_s) = G_s[S_s(R_s)]^2 + G_\sigma[S_\sigma(R_s)]^2 + \gamma_p G_\pi[S_\pi(R_s)]^2, \tag{12}$$

where G_s, G_σ, and G_π are dimensionless parameters of the model; $\gamma_2 = 3/2$, $\gamma_4 = 1/3$, $\gamma_6 = -3/2$; the overlap integrals $S_s = \langle 4f, m=0 | 2s \rangle$, $S_\sigma = \langle 4f, m=0 | 2p, m=0 \rangle$, $S_\pi = \langle 4f, m=1 | 2p, m=1 \rangle$ have been computed using the radial $4f$ wave function of the Er^{3+} ion from Ref. 26 and the $2s, 2p$ wave functions of the F^- ion given in Ref. 27. Dependencies of the overlap integrals on the interionic distance R (in atomic units) can be approximated by the following expressions:[28]

$$S_s = 2.3097 \exp(-1.2865R);$$
$$S_\sigma = 0.6908 \exp(-0.9117R);$$
$$S_\pi = 1.3121 \exp(-1.1785R).$$

Uniform spherical polynomials $W_{p,\alpha}^k$ of the $(p+1)$th power are defined by the following equations:

$$W_{p,\alpha}^k \frac{a_{p+1,0}}{a_{p,0}} \frac{(p+1)}{R^{p+2}} = -\frac{\partial}{\partial X_\alpha} \left(\frac{O_p^k}{R^{p+1}} \right) \tag{13}$$

and can be put down as linear combinations of polynomials $O_{p+1}^{k'}$:

$$b_{p,k} W_{p,x}^k = \frac{1}{2} \text{sgn}\, k (b_{p+1,k+1} O_{p+1}^{k+1} - b_{p+1,k-1} O_{p+1}^{k-1}),$$
$$|k + 1/2| \geq 3/2,$$

$$b_{p,k} W_{p,y}^k = \frac{1}{2} \text{sgn}\, k (b_{p+1,-k+1} O_{p+1}^{-k+1} + b_{p+1,-k-1} O_{p+1}^{-k-1}),$$
$$|k - 1/2| \geq 3/2,$$

$$b_{p,0} W_{p,x}^0 = b_{p+1,1} O_{p+1}^1, \quad b_{p,0} W_{p,y}^0 = b_{p+1,-1} O_{p+1}^{-1},$$

$$b_{p,k} W_{p,z}^k = b_{p+1,k} O_{p+1}^k,$$

$$b_{p,-1} W_{p,x}^{-1} = b_{p,1} W_{p,y}^1 = \frac{1}{2} b_{p+1,-2} O_{p+1}^{-2}.$$

The numerical factors $b_{p,k}$ are presented in Ref. 13.

In the present work, we employed the simplest version of the ECM with only one phenomenological parameter $G_s = G_\sigma = G_\pi = 7.02$ obtained from a comparison of the calculated and measured crystal-field splittings of the ground multiplet. Calculations were greatly simplified by taking into account interactions of the Er^{3+} ion with its nearest neighbors only, namely, with eight F^- ions. Their coordinates, relative to the Er^{3+} ion, are $[\pm ay, \pm a(0.5-x), c(z-0.25)]$, $[\pm a(y-0.5), \pm a(0.5-x), -cz]$, $[\pm a(x-0.5), \pm a(y-0.5), cz]$, $[\pm a(x-0.5), \pm ay, -c(z-0.25)]$. The following values of the structure constants of the lattice were used:[21,29] $a=0.5168$ nm, $c=1.0731$ nm, $x=0.2821$, $y=0.1642$, $z=0.081\,51$. Contributions due to these ligands to the crystal-field parameters are given in column 2 of Table II. The probability of the one-phonon transition between the electronic initial (i) and final (f) states with energy gap $\hbar\omega_{if}>0$ can be presented as

$$W_{if} = \frac{2}{\hbar} \sum_{s\alpha s'\beta} \langle f|V_\alpha(s)|i\rangle \mathrm{Im}\, g_{\alpha\beta}(ss'|\omega)\langle i|V_\beta(s')|f\rangle$$
$$\times [n(\omega_{if})+1], \qquad (14)$$

where $n(\omega)$ is the phonon occupation number and $g_{\alpha\beta}(ss'|\omega)$ are the linear combinations of the lattice Green's functions for the differences between displacements of ligands and the Er^{3+} ion:

$$g_{\alpha\beta}(ss'|\omega) = G_{\alpha\beta}(s,s'|\omega) - G_{\alpha\beta}(s,\mathrm{Er}|\omega) - G_{\beta\alpha}(s',\mathrm{Er}|\omega)$$
$$+ G_{\alpha\beta}(\mathrm{Er},\mathrm{Er}|\omega). \qquad (15)$$

We performed a calculation of the relaxation rates for all the crystal-field sublevels within the manifolds of $^4I_{11/2}$ and $^4I_{13/2}$ multiplets using the phonon Green's functions of the perfect and locally perturbed (isolated impurity centers at the Y^{3+} sites) LiYF$_4$ crystal lattices. The Green's function matrix for the locally perturbed crystal can be written down through the Green's function $\mathbf{G}^0$ of the perfect crystal. We have considered only the mass defect effect on the local dynamical properties of the lattice due to a substitution of Er for Y. In this case,

$$\mathbf{G} = \mathbf{G}^0 - \mathbf{G}^0(1 + \delta\mathbf{m}\omega^2\mathbf{G}_0)^{-1}\delta\mathbf{m}\omega^2\mathbf{G}^0, \qquad (16)$$

where, in the site representation, $\delta\mathbf{m}$ is the diagonal matrix with three nonzero elements corresponding to coordinates of the impurity ion and equal to the difference between the masses of erbium and yttrium. Because of the local S_4 symmetry, we had to deal with a simple one-dimensional problem. Frequencies and polarization vectors of phonons in the LiYF$_4$ crystal were obtained at 8000 points in the irreducible part of the Brillouin zone using the rigid ion model of lattice dynamics derived in Ref. 21 on the basis of neutron scattering data. Imaginary parts of the Green's functions were calculated by numerical integration over the Brillouin zone and real parts were obtained with the Cauchy relations. Examples of calculated spectral densities of the displacement-displacement correlation functions are given in Fig. 3.

Matrix elements of electronic operators $V_\alpha(s)$ were calculated with the eigenfunctions of the Hamiltonian (1). The inverse lifetimes of the crystal-field sublevels
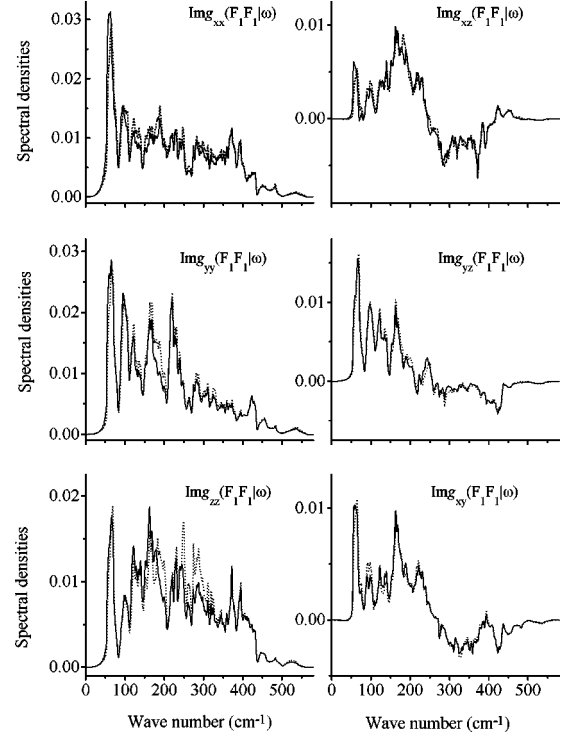
FIG. 3. Spectral densities of displacement-displacement correlation functions $\mathrm{Im}\, g_{\alpha\beta}(F_1,F_1|\omega)$ in crystals of LiYF$_4$:Er^{3+} (solid curves) and LiYF$_4$ (dotted curves). The radius vector of the fluorine ion F_1 relative to Er^{3+} (Y^{3+}) ion has the components $[ay, a(0.5-x), c(z-0.25)]$.

$$1/\tau_i = W_i = \sum_f W_{if} \qquad (17)$$

determine the widths of corresponding absorption lines. At low temperatures, the sum in Eq. (17) is over states f that belong to the same multiplet as the crystal-field level i, with lower energies. Results of calculations of the linewidths $\Delta E_i = W_i/2\pi c$ with the perturbed Green's functions at the temperature of 5 K are given in Table I. It should be noted that the mass defect perturbation of the lattice induces relatively small (up to 10%) changes of the one-phonon relaxation rates. It is seen from Table I that despite many simplifying approximations there is a good correlation between the measured linewidths and the estimated relaxation rates (up to a factor of 3) except for the widths of the $\Gamma_{56}^{(2)}$ and $\Gamma_{56}^{(3)}$ sublevels in the $^4I_{11/2}$ multiplet. In these two cases, we obtained certainly overestimated relaxation rates in channels $\Gamma_{56}^{(2)} \to \Gamma_{78}^{(1)}$ and $\Gamma_{56}^{(3)} \to \Gamma_{56}^{(1)}$ with gaps of 59.7 and 62.4 cm^{-1}, respectively, which coincide with the first large maximum in the spectral densities of the lattice correlation functions (see Fig. 3). It seems probable that substitution of trivalent rare-earth ions for Y^{3+} ions induces local enhancement of force constants and, correspondingly, essential redistributions of the spectral densities of the relative displacements of the rare-earth ion and its ligands.

V. CONCLUSION

Using high-resolution Fourier-transform spectroscopy we accurately measured the energies of all the crystal-field lev-

els within the $^4I_{13/2}$ and $^4I_{11/2}$ multiplets and of the three lowest excited states of $^4I_{15/2}$ in LiYF$_4$:Er and analyzed the widths of spectral lines. We were able to resolve the hyperfine structures of infrared transitions of the ^{167}Er^{3+} ion. The crystal-field energies and hyperfine structures calculated with the crystal-field parameters and hyperfine constants known from the literature reproduced the measured spectra rather well. We performed the calculations of the one-phonon relaxation rates in the framework of the exchange charge model and using a realistic model of the lattice dynamics. Results of the calculations were shown to agree within an order of magnitude with measured homogeneous linewidths of zero-phonon transitions between the ground state and sublevels of the $^4I_{13/2}$ and $^4I_{11/2}$ multiplets at low temperatures.

[1] M. V. Petrov and A. M. Tkachuk, Opt. Spektrosk. **45**, 147 (1978) [Opt. Spectrosc. **45**, 81 (1978)].

[2] F. Auzel, S. Hubert, and D. Meichenin, Appl. Phys. Lett. **54**, 681 (1989).

[3] M. R. Brown, K. G. Roots, and W. A. Shand, J. Phys. C **2**, 593 (1969).

[4] S. M. Kulpa, J. Phys. Chem. Solids **36**, 1317 (1975).

[5] H. P. Christensen, Phys. Rev. B **19**, 6564 (1979).

[6] G. M. Renfro, J. C. Windscheif, W. A. Sibley, and R. F. Belt, J. Lumin. **22**, 51 (1980).

[7] S. Hubert, D. Meichenin, B. W. Zhou, and F. Auzel, J. Lumin. **50**, 7 (1991).

[8] F. Auzel and Y. Chen, J. Lumin. **65**, 45 (1995).

[9] M. A. Couto dos Santos, E. Antic-Fidancev, J. Y. Gesland, J. C. Krupa, M. Lemaître-Blaise, and P. Porcher, J. Alloys Compd. **275-277**, 435 (1998).

[10] N. I. Agladze and M. N. Popova, Solid State Commun. **55**, 1097 (1985).

[11] N. I. Agladze, M. N. Popova, G. N. Zhizhin, V. J. Egorov, and M. A. Petrova, Phys. Rev. Lett. **66**, 477 (1991).

[12] R. M. Macfarlane, A. Cassanho, and R. S. Meltzer, Phys. Rev. Lett. **69**, 542 (1992).

[13] B. Z. Malkin, in *Spectroscopy of Solids Containing Rare-Earth Ions*, edited by A. A. Kaplyanskii and R. M. Macfarlane (North-Holland, Amsterdam, 1987), p. 13.

[14] N. I. Agladze, H. S. Bagdasarov, E. A. Vinogradov, V. I. Zhekov, T. M. Murina, M. N. Popova, and E. A. Fedorov, Kristallografiya **33**, 912 (1988).

[15] A. A. Kaminskii, *Crystalline Lasers: Physical Processes and Operating Schemes* (CRC Press, Boca Raton, FL, 1996).

[16] J. P. Sattler and J. Nemarich, Phys. Rev. B **4**, 1 (1971).

[17] M. A. H. McCausland and I. S. Mackenzie, Adv. Phys. **28**, 305 (1979).

[18] A. Abragam and B. Bleaney, *Electron Paramagnetic Resonance of Transition Ions* (Clarendon Press, Oxford, 1970).

[19] V. C. Das and A. K. Ray Chaudhuri, J. Phys. C **6**, 1385 (1973).

[20] L. A. Bumagina, V. I. Krotov, B. Z. Malkin, and A. Kh. Khasanov, Zh. Éksp. Teor. Fiz. **80**, 1543 (1981) [Sov. Phys. JETP **53**, 792 (1981)].

[21] S. Salaun, A. Bulou, M. Rousseau, B. Hennion, J. Y. Gesland, J. Phys.: Condens. Matter **9**, 6957 (1997).

[22] M. P. Davidova, S. B. Zdanovitch, B. N. Kazakov, S. L. Korableva, and A. L. Stolov, Opt. Spektrosk. **42**, 577 (1977) [Opt. Spectrosc. **42**, 327 (1977)].

[23] A. A. Antipin, L. A. Bumagina, B. Z. Malkin, and R. M. Rakhmatullin, Fiz. Tverd. Tela (Leningrad) **23**, 2700 (1981) [Sov. Phys. Solid State **23**, 1583 (1981)].

[24] A. V. Vinokurov, B. Z. Malkin, A. I. Pominov, A. L. Stolov, Fiz. Tverd. Tela. (Leningrad) **30**, 801 (1988) [Sov. Phys. Solid State **30**, 459 (1988)].

[25] R. M. Sternheimer, M. Blume, and R. F. Peierls, Phys. Rev. **173**, 376 (1968).

[26] A. J. Freeman and R. E. Watson, Phys. Rev. **127**, 2058 (1962).

[27] E. Clementi and A. D. McLean, Phys. Rev. **133**, A419 (1964).

[28] T. T. Basiev, Yu. V. Orlovskii, K. K. Pukhov, V. B. Sigachev, M. E. Doroshenko, and I. N. Vorob'ev, J. Lumin. **68**, 241 (1996).

[29] P. Blanchfield and G. A. Saunders, J. Phys. C **12**, 4673 (1979).